11-12-2012

Blt1 and Mid1 Provide Overlapping Membrane Anchors To Position the Division Plane in Fission Yeast

Merce Guzman-Vendrell
Universite Pierre et Marie Curie (Paris VI)

Suzanne Baldissard
Dartmouth College

Maria Almonacid
Universite Pierre et Marie Curie (Paris VI)

Adeline Mayeux
Universite Pierre et Marie Curie (Paris VI)

Anne Paoletti
Universite Pierre et Marie Curie (Paris VI)

See next page for additional authors

MCB
Journals.ASM.org

Blt1 and Mid1 Provide Overlapping Membrane Anchors To Position the Division Plane in Fission Yeast

Mercè Guzman-Vendrell,[a,b] Suzanne Baldissard,[c] Maria Almonacid,[a,b]* Adeline Mayeux,[a,b] Anne Paoletti,[a,b] James B. Moseley[c]

Institut Curie, Centre de Recherche, Paris, France[a]; CNRS UMR144, Paris, France[b]; Department of Biochemistry, Geisel School of Medicine at Dartmouth, Hanover, New Hampshire, USA[c]

Spatial control of cytokinesis is essential for proper cell division. The molecular mechanisms that anchor the dynamic assembly and constriction of the cytokinetic ring at the plasma membrane remain unclear. In the fission yeast *Schizosaccharomyces pombe*, the cytokinetic ring is assembled in the cell middle from cortical node precursors that are positioned by the anillin-like protein Mid1. During mitotic entry, cortical nodes mature and then compact into a contractile ring positioned in the cell middle. The molecular link between Mid1 and medial cortical nodes remains poorly defined. Here we show that Blt1, a previously enigmatic cortical node protein, promotes the robust association of Mid1 with cortical nodes. Blt1 interacts with Mid1 through the RhoGEF Gef2 to stabilize nodes at the cell cortex during the early stages of contractile ring assembly. The Blt1 N terminus is required for localization and function, while the Blt1 C terminus promotes cortical localization by interacting with phospholipids. In cells lacking membrane binding by both Mid1 and Blt1, nodes detach from the cell cortex and generate aberrant cytokinetic rings. We conclude that Blt1 acts as a scaffolding protein for precursors of the cytokinetic ring and that Blt1 and Mid1 provide overlapping membrane anchors for proper division plane positioning.

Cell division requires the spatial and temporal coordination of many cellular activities. During cytokinesis, the final act of the cell cycle, a contractile actomyosin ring constricts to separate the two daughter cells. The contractile ring must be properly assembled and positioned to ensure equal segregation of cellular materials to each daughter cell. The contracting cytokinetic ring maintains association with the cell cortex, which undergoes dramatic remodeling and membrane bending during this process. The mechanisms that position and anchor components of the cytokinetic ring in the plasma membrane have been the subject of intense study, as defects in this process can lead to a range of cellular defects and disease states (1–4).

Many insights into eukaryotic cytokinesis have come from work on the fission yeast *Schizosaccharomyces pombe* (1, 5). These rod-shaped cells grow in a linear manner at the cell ends and then position the contractile ring precisely in the cell middle at division. This positioning occurs through the combination of inhibitory signals emanating from the cell ends and positive cues from the nucleus in the cell middle. These positional cues act largely through the protein Mid1, which is similar to anillin in metazoans (6, 7). During interphase, Mid1 localizes to the nucleus and to a band of cortical nodes that are positioned in the cell middle. These interphase nodes are organized by the protein kinase Cdr2 and are spatially restricted to the cell middle by inhibitory cues from the cell tips (8–12). During interphase, these cortical nodes also contain a cell cycle regulatory network that couples mitotic entry with cell size (11, 13). Proteomic studies have revealed additional node components, such as the protein Blt1, the RhoGEF Gef2, and the kinesin Klp8 (11), which remain largely uncharacterized. Blt1, Gef2, and Klp8 all localize to cortical nodes and to the contractile cytokinetic ring, but their absence does not lead to obvious cytokinetic defects. This suggests the possibility that they function redundantly with other cytokinetic proteins.

As the cell enters mitosis, many cytokinesis proteins, including type II myosin and actin-binding proteins, are recruited to medial cortical nodes, which subsequently condense to form the contractile ring (5). Mid1 is required for the localization of cytokinesis proteins to these cortical nodes (14–21), and *mid1* mutants display severely misplaced contractile rings and septa (6, 7). These findings indicate that recruitment of Mid1 to cortical nodes is a key step in the assembly and positioning of cytokinesis. However, the molecular mechanisms that anchor Mid1 at cortical nodes in the plasma membrane remain unclear. The carboxyl terminus of Mid1 contains a membrane-binding amphipathic helix, but deletion of this helix does not greatly impair Mid1 localization or function. Rather, the amino-terminal half of Mid1 (Mid1-Nter; residues 1 to 506) is necessary and largely sufficient for Mid1 function and localization to cortical nodes (22).

In this study, we found that the node protein Blt1 is required for the localization and function of Mid1-Nter. Further, the interaction of Blt1 with Mid1 is mediated by the RhoGEF Gef2. Using a structure-function approach, we identified an N-terminal domain of Blt1 that is necessary for localization to medial cortical nodes and function. A separate C-terminal membrane-binding domain functions in parallel to the Mid1 membrane-binding helix to anchor Mid1 at the medial cortex and promote cell division in the cell middle. Our findings indicate that the assembly of the cytokinetic ring by cortical precursors requires multiple interactions of cortical node components with the plasma membrane.

Received 19 September 2012 **Returned for modification** 18 October 2012
Accepted 5 November 2012

Published ahead of print 12 November 2012

Address correspondence to Anne Paoletti, Anne.Paoletti@curie.fr, or James B. Moseley, james.b.moseley@dartmouth.edu.

* Present address: Maria Almonacid, CIRB, Collège de France, Paris, France.

Supplemental material for this article may be found at http://dx.doi.org/10.1128/MCB.01286-12.

doi:10.1128/MCB.01286-12

MATERIALS AND METHODS

Strains and plasmids. All *S. pombe* strains used were isogenic to 972 and are listed in Table S1 of the supplemental material. Standard *S. pombe* molecular genetics techniques and media were used (23). Strains were selected from genetic crosses by random spore analysis or tetrad dissection.

The Mid1 plasmids used in this study were derived from integrative vector pJK148 (24). pAP93, pAP146, pAP159, pSM26, pMA32, and pMA34 were described previously (8, 22, 25). Of note, pAP93 (pmid1-mid1) contains a point mutation at amino acid (aa) 6 of Mid1, which does not alter Mid1 function (A. Paoletti, unpublished data). pMA15 (pmid1-GFP-mid1-300-350) was obtained by fusing a NotI-BamHI PCR product containing Mid1 aa 300 to 350 to pSM26 (containing pmid1 and the green fluorescent protein [GFP] gene) cut with similar enzymes. pMG60 (pmid1-GST-mid1-300-450) was obtained by subcloning a XhoI-NotI fragment containing the glutathione *S*-transferase (GST) gene from pDS473 (a generous gift from S. Forsburg) and a NotI-SacI fragment from pMA16 (8), containing Mid1 aa 300 to 450 followed by the nmt1 stop, into pAP140 (22), which had been cut by SalI and SacI. Plasmids were linearized by NruI in the *leu1* gene and then integrated into the genome of *mid1*Δ *leu1-32*, *mid1*Δ *blt1*Δ *leu1-32*, *mid1*Δ *blt1-mEGFP leu1-32*, and *mid1*Δ *blt1-mCherry leu1-32* strains, due to the tight genetic linkage between *leu1* and *blt1* loci. Transformations were performed using the lithium acetate-dimethyl sulfoxide method (26).

To introduce the Mid1-Nter construct at the *mid1* locus, 500-bp fragments corresponding to the end of the Mid1 N terminus (aa 1 to 506) and *mid1* terminator (*tmid1*) were amplified by PCR using oligonucleotides terminated by sequences specific for the pFa6a-hphMX6 plasmid (27). These fragments were used to produce a PCR product encoding *mid1-Nter-tADH-NatMX-tmid1* by using Primestar enzyme (TaKaRa). This PCR product was integrated into strains AP3906 and AP3907 to produce strains AP3924 and AP3925.

An integration plasmid for Cdr2 constructs was produced by insertion of 1 kb of the *cdr2* promoter (*pcdr2*) and terminator (*tcdr2*) into pFA6a-GFPkanMX6 (26) between SalI and BamHI sites and SacI and SpeI sites, respectively. The *cdr2*$^+$ open reading frame (ORF) was then inserted upstream of GFP(S65T) between BamHI and PacI to create pSR34. Finally, GFP was replaced between PacI and AscI sites by GFP-CAAX, amplified by PCR by using a reverse oligonucleotide encoding the last 19 amino acids of Mod5, including a prenylation motif (KPPKKKGSKLEKFCCILM [28]) in frame with GFP. NotI fragments of pSR34 and pSR58 containing *pcdr2-cdr2-GFP-tADH-kanMX-tcdr2* or *pcdr2-cdr2-GFP-CAAX-tADH-kanMX-tcdr2*, respectively, were transformed in a *cdr2*Δ::*natMX6 leu1-32* *h*$^-$ strain (AP2804) to produce strain AP3177 and AP3909. Geneticin-resistant and CloNat-sensitive clones were checked by PCR for proper genome integration of Cdr2 constructs.

To map Blt1 localization domains, Blt1 fragments were PCR amplified and subcloned into the NdeI-BamHI sites of pREP41-GFPN (29). These plasmids were transformed into strain JM429; overexpression was induced by growth in medium lacking thiamine for at least 24 h at 25°C.

To integrate *blt1*Δ*1*-mCherry, a fragment containing *pblt1-blt1-mCherry-tadh1* was PCR amplified from strain JM1598 and subcloned into integrative vector pJK210. The StuI sites in mCherry were removed by silent mutations using site-directed mutagenesis. The coding sequence for Blt1 amino acids 2 to 78 was deleted by site-directed mutagenesis to generate *blt1*Δ*1*-mCherry. Both the full-length pJK210-*pblt1-blt1-mCherry-tadh1* (pJM584) and the truncated pJK210-*pblt1-blt1*Δ*1-mCherry-tadh1* (pJM585) plasmids were linearized by digestion with StuI, and then integrated into the *ura4-294* allele. The resulting integrants were combined with *blt1*Δ::natR, meaning that Blt1-mCherry or *blt1*Δ*1*-mCherry was expressed as the sole genomic copy and under the control of the endogenous promoter. To generate blt1Δ5 mutants, we integrated mCherry-natR or GFP-kanMX6 at the endogenous *blt1*$^+$ locus after the codon for amino acid 575 by using the pFA6a system (26).

Coimmunoprecipitation and lipid binding experiments. For coimmunoprecipitations, 200 ml of cells were grown to an optical density at 595 nm of 1 at 30°C in YE5S medium concentrated 2 times compared to regular YE5S medium (YE5S2×). The cells were first washed with 1 ml of Stop buffer (NaCl at 150 mM, NaF at 50 mM, NaEDTA at 10 mM, NaN_3 at 1 mM), then resuspended in 600 μl 1D buffer (HEPES at 50 mM [pH 7.5], NaCl at 100 mM, EDTA at 1 mM, NP-40 at 1%, β-glycerophosphate at 20 mM, NaF at 50 mM, Na_3VO_4 at 0.1 mM, phenylmethylsulfonyl fluoride at 1 mM complemented with complete EDTA-free antiprotease tablets [Roche]) together with 600 μl of glass beads and broken using a FastPrep FP120A instrument (Qbiogene; two cycles of 40 s at maximum speed). Lysates were then spun at 10,000 × *g* for 10 min at 4°C, and supernatants were recovered. Soluble extracts were incubated with anti-mouse IgG magnetic beads (M-280 Dynal; Invitrogen) coupled to 6 μg of anti-GFP monoclonal antibody (MAb; Roche), antihemagglutinin (anti-HA) MAb 12CA5 (Roche), or anti-myc MAb 9E10 (Roche) for 2 h at 4°C; then, the beads were washed five times with 1D buffer and the beads were resuspended in SDS-PAGE sample buffer. Immunoprecipitation (IP) samples and soluble extracts were submitted to SDS-PAGE and transferred to nitrocellulose membranes. Western blot assays were performed with anti-GFP MAb (1/500; Roche), and anti-Mid1 affinity-purified Ab (1/200 [22]). Secondary antibodies were coupled to peroxidase (Jackson ImmunoResearch) or to alkaline phosphatase (Promega). Signal quantification was performed in Metamorph. The signals of coimmunoprecipitated proteins were normalized relative to the protein concentration in the input and the amount of primarily precipitated protein.

For lipid-binding assays, GFP-Blt1- and GFP-blt1Δ5-containing extracts were prepared by bead beating in lysis buffer (1× Tris-buffered saline, 0.5% Triton X-100, 1 mM EDTA, protease inhibitor cocktail [Roche]) and clarified by centrifugation at 16,000 × *g* for 10 min at 4°C. Clarified extracts were diluted in blocking buffer and incubated with membrane lipid strips (Echelon Bioscience) according to the manufacturer's protocol. Lipid strips were probed with anti-GFP antibodies (11).

Microscopy. Cells were grown exponentially at 25°C in YE5S or EMM4S, except for the cells shown in Fig. S1 in the supplemental material, which were grown overnight in patches on YE5S plates to limit autofluorescence. Cells were imaged in liquid medium under a coverslip using four microscopes, as follows.

For the images in Fig. 9 and Fig. S1, S3, and S11 in the supplemental material, microscopy was performed on a DMRXA2 upright microscope (Leica Microsystems) equipped with a 100×/1.4-numerical-aperture (NA) Plan Apochromat objective and a Coolsnap HQ charge-coupled-device (CCD) camera (Roper). In the image in Fig. S3, 5 interphase cells of similar lengths (12.9 to 13.5 μm) were randomly selected from differential interference contrast (DIC) images. GFP fluorescence along the cortex from tip to tip was analyzed by using the line scan tool of Metamorph software (4 pixels in width). Background values were subtracted before plotting.

For the images in Fig. 1A and 8A and Fig. S2, S9, and S10 in the supplemental material, we used a Nikon Eclipse TE2000-U microscope equipped with a 100×/1.45-NA oil immersion objective, a PIFOC objective stepper, a Yokogawa CSU22 confocal unit, and a Roper HQ2 CCD camera. For time-lapse movies in Fig. 8A and Fig. S10 in the supplemental material, stacks of 7 planes spaced by 1 μm were acquired every 2 min (binning 2, gain 3; 500 ms at 15% laser power for both GFP and mCherry [Fig. 8A], or 20% of GFP laser power [Fig. S11]). In Fig. 1A and also Fig. S2 and S9 in the supplemental material, individual stacks were taken using a laser power of 60% for GFP and 80% for mCherry, and 13 planes were taken with a step size of 0.5 μm and 300-ms exposure.

For Fig. 1B, 3, 4, 6, and 7 and Fig. S5 to S7 in the supplemental material, images were obtained on a DeltaVision imaging system and processed by iterative deconvolution as described previously (30).

For Fig. 5, cells were imaged by spinning disk confocal microscopy as described previously (30). Images were analyzed in ImageJ or Metamorph.

RESULTS

Blt1 is required for division plane positioning when Mid1 binding to membranes is impaired. The N-terminal half of Mid1 localizes to the nucleus, cortical nodes, and the cytokinetic ring and division septum (22). Cells expressing Mid1-Nter lack the C-terminal half of Mid1, making them functionally dependent on interactions made by Mid1-Nter. The localization of Mid1-Nter to medial cortical nodes and its function are fully disrupted in *cdr2*Δ cells, which lack cortical nodes in the cell middle. Similar defects are observed when a Mid1-Nter site necessary for Mid1 interaction with Cdr2 is deleted (aa 400 to 450). Interestingly, deletion of another region of Mid1-Nter (aa 300 to 350) yields the same phenotype without impairing the Mid1-Cdr2 interaction (8), suggesting that other components of cortical nodes may be required for the cortical recruitment and function of Mid1-Nter.

Since Blt1 and Mid1 coimmunoprecipitate in cell extracts (11) and Blt1 colocalized with Mid1-Nter in cortical nodes during interphase and at the cytokinetic ring (see Fig. S1 in the supplemental material), we tested the possibility that Blt1 recruits Mid1-Nter to cortical nodes. We found that in the absence of Blt1, Mid1-Nter localized to the nucleus but was largely absent from cortical nodes (Fig. 1A and B). These Mid1-Nter *blt1*Δ cells displayed misplaced cytokinetic rings and septa similar to *mid1*Δ (Fig. 1A). Only a small proportion of Mid1-Nter and *blt1*Δ single mutant cells displayed misplaced septa, consistent with previous results (11, 22), but septa were misplaced in nearly all Mid1-Nter *blt1*Δ double mutant cells (Fig. 1C). This synthetic defect indicated that Blt1 functions to recruit Mid1 to the cell cortex for cytokinesis in the absence of the Mid1 C terminus.

The C terminus of Mid1 contains an amphipathic helix that associates with membranes at the cell cortex. Mutation of this helix (*mid1-helix**) leads to only minor cytokinesis defects similar to those resulting from deletion of the entire C terminus in the Mid1-Nter construct. We hypothesized that this amphipathic helix and Blt1 represent overlapping mechanisms that attach Mid1 to the cell cortex. Consistent with this model, combining *mid1-helix** and *blt1*Δ mutations led to severe defects in the position of division septa (Fig. 1C). We concluded that Mid1 associates with the cortex to position the cytokinetic ring through both its amphipathic helix and interaction with Blt1 and Cdr2 at medial cortical nodes.

Mid1(300-350) mediates interaction with Blt1 through Gef2. We next investigated the physical interaction between Mid1 and Blt1 at the cell cortex. Deletion of Mid1 300-350 dramatically reduced the Mid1 interaction with Blt1 (Fig. 2A), indicating that residues 300 to 350 of Mid1 are required for association with Blt1. Indeed, deletion of these residues in Mid1-Nter abolished localization to cortical nodes and the contractile ring (see Fig. S2 in the supplemental material), as previously reported (8, 31). Interestingly, we also found that Blt1-mEGFP was less concentrated in the cell middle in *mid1*Δ*300-350* cells (see Fig. S3 in the supplemental material), suggesting that the interaction of Mid1 and Blt1 may reciprocally promote their localization to medial cortical nodes.

Recruitment of Mid1-Nter to cortical nodes also depends on Gef2 (31), a putative Rho GTPase GEF protein. Similar to Mid1-Nter, the localization of Gef2 to interphase cortical nodes requires Blt1 (11, 31). Thus, we considered that Gef2 might bridge the interaction between Blt1 and Mid1-Nter. Indeed, coimmunoprecipitation of Blt1 and Mid1 was abolished in *gef2*Δ cells (Fig. 2B).

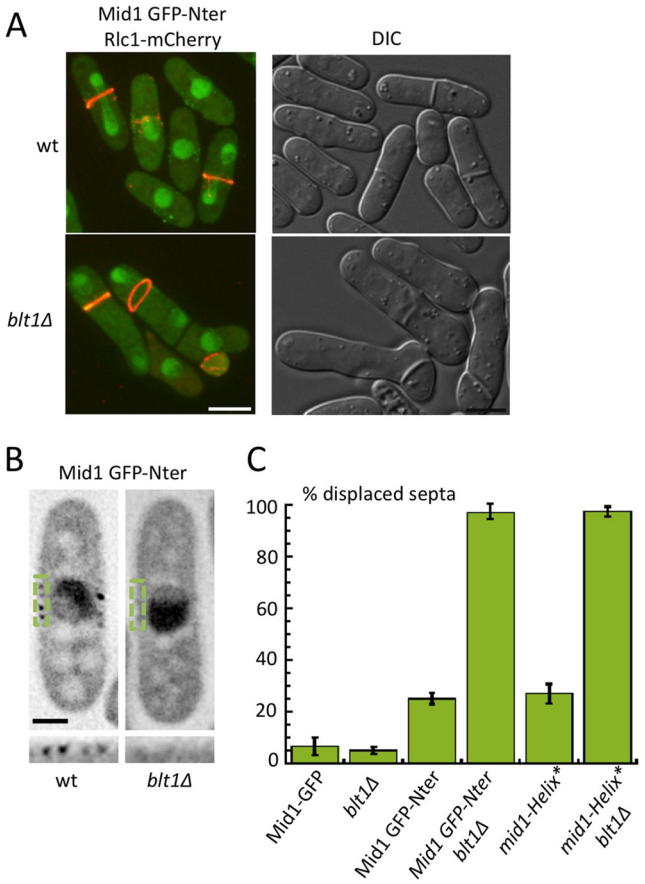

FIG 1 Blt1 promotes Mid1-Nter localization and function. (A, left) Localization of the Mid1 N terminus (Mid1 GFP-Nter) and Rlc1-mCherry in wild-type and *blt1*Δ cells deleted for endogenous *mid1*. Strains used were AP3900 and AP3903. Images are maximum projections of spinning disc confocal *z*-series. (Right) DIC images of the same mutants. Strains were AP998 and AP2172. Bar, 5 μm. (B) Mid1 GFP-Nter is largely absent from cortical nodes in *blt1*Δ cells. Images are deconvolved inverted single focal planes, and the bottom row shows magnified views of green, boxed regions. Bar, 2 μm. Strains used were AP998 (4 nodes/cell; $n = 77$ cells) and AP2172 (0.5 node/cell; $n = 64$ cells). (C) Percentage of displaced septa for the indicated genotypes (strains AP528, AP998, JM429, AP2172, AP583, and AP2335). Bars represent means ± standard deviations (error bars) from two separate experiments ($n > 300$ cells in each experiment).

In contrast, Gef2 coimmunoprecipitated with Mid1 in both wild-type and *blt1*Δ cells (Fig. 2C). This suggested that Blt1 associates with Mid1-Nter indirectly through Gef2, which may act as an adaptor protein in cortical nodes.

To further investigate these physical interactions, we identified by coimmunoprecipitation a minimal fragment of Mid1 that associated with Blt1 and Gef2 (see Fig. S4A in the supplemental material). Similar to the full-length protein, Mid1(300-450) associated with Blt1 in wild-type but not *gef2*Δ cell extracts, while the same fragment interacted with Gef2 independently of Blt1 (see Fig. S4B and C). Furthermore, we found that Mid1 residues 300 to 350 were sufficient for localization to the cytokinetic ring and septum in cells, and this localization was lost in *blt1*Δ cells (see Fig. S2C and D in the supplemental material). These combined data indicate that residues 300 to 450 of Mid1 interact with Blt1 indirectly through Gef2 to promote Mid1-Nter cortical localization,

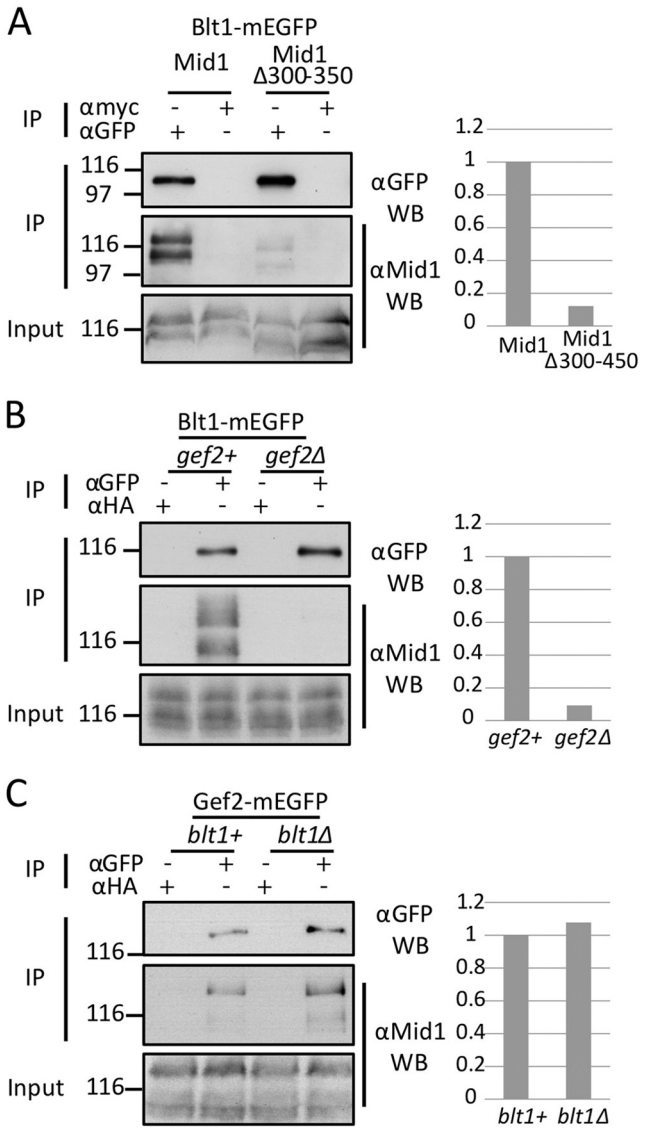

FIG 2 Mid1 interacts with Blt1 through Gef2. (A) Coimmunoprecipitation assay results between Blt1-mEGFP and the indicated Mid1 construct. Immunoprecipitation was performed with an anti-GFP MAb, or with an anti-HA or anti-myc MAb as negative controls. Input and IP samples were probed with anti-Mid1 antibodies. Normalized signal quantification from two independent experiments is shown on the right. Strains used were AP3490 and AP3491. (B and C) Coimmunoprecipitation assay results between Blt1 (B) or Gef2 (C) and Mid1 in *gef2*$^+$ or *gef2*Δ or *blt1*$^+$ *or blt1*Δ backgrounds, respectively. Immunoprecipitation was performed as for panel A. Normalized signal quantification from two independent experiments is shown on the right. Strains used were JM151, AP3872, JM365, and AP3873.

contractile ring localization, and function. This raises the possibility that Blt1 acts as a cortical anchor for Mid1-Nter, with Gef2 functioning to bridge Blt1-Mid1 interactions either directly or indirectly.

Blt1 associates with the cell cortex. Based on our evidence that Blt1 anchors Mid1-Nter at cortical nodes, we hypothesized that Blt1 is a lipid-binding scaffold protein for cortical nodes and the contractile ring at the plasma membrane. Indeed, Blt1 localizes to cortical structures (nodes and contractile ring) throughout the cell cycle, and it also remains at the cell cortex upon disruption of nodes by *cdr2*Δ (11). In support of Blt1 as a membrane scaffold, we observed Blt1-mEGFP in a contractile ring that was external of the contractile myosin ring, marked by Rlc1-mRFP, during cytokinesis (see Fig. S5A and B in the supplemental material). This organization was present in all cells examined ($n = 20$) and was maintained when we imaged Blt1-mCherry Rlc1-mEGFP cells, indicating that it was not due to the respective fluorophores (see Fig. S5A). This places Blt1 in a position to link the membrane with components of the contractile ring.

To investigate the Blt1 association with the cell cortex further, we increased the expression of GFP-Blt1. When overexpressed by the strong P3nmt1 promoter, GFP-Blt1 coated the cell periphery (see Fig. S5C and D in the supplemental material). This indicated that Blt1 association with the cell cortex is not saturable, as expected for a lipid-binding protein. Importantly, the localization of GFP-Blt1 to the cell periphery was also independent of Cdr2, which recruits endogenously expressed Blt1 to medial cortical nodes (see Fig. S5E) (11). These results suggest that Blt1 may interact with the lipid bilayer. Despite its abundance at the cell cortex, GFP-Blt1 was excluded from the cortex at growing cell ends, as marked by the cell wall dye blankophor (see Fig. S5C). In addition, GFP-Blt1 localized to the nongrowing end of monopolar mutants, indicating that its exclusion at cell ends is not due to membrane curvature or geometry (see Fig. S5E). Rather, this was reminiscent of the previous studies that have shown the exclusion of other proteins at sites of cell growth (9, 11–13), perhaps due to a different lipid composition and/or membrane flux at these sites.

Domain analysis of Blt1. The only sequence-predicted domain in Blt1 was a leucine zipper motif between residues 488 to 575. To search for additional functional domains, we generated a panel of Blt1 truncation mutants that were expressed from multicopy plasmids under the control of the medium-strength P41nmt1 promoter in *blt1*Δ cells. In the repressed state, full-length Blt1 expressed by this promoter localized similarly to the endogenous protein. When induced, this promoter drove overexpression of Blt1, leading to localization throughout the nongrowing cell cortex (Fig. 3). We used this expression system to determine the localization of 12 truncation mutants under endogenous and overexpression conditions (Fig. 3; see also Fig. S6 in the supplemental material).

Upon overexpression, we observed a strong localization at the cell periphery for all constructs containing a C-terminal domain that encompassed residues 575 to 700 (e.g., *blt1*Δ*1* and *blt1*Δ*4* [Fig. 3; see also Fig. S6 in the supplemental material]). In contrast, constructs lacking this C-terminal domain (e.g., *blt1*Δ*5*) were not found at the cell periphery upon overexpression. This means that a C-terminal 125-amino-acid domain is both required and sufficient for Blt1 association with the cell periphery. Interestingly, Blt1 localization to medial cortical nodes at endogenous expression levels appears to be independent of the C terminus. For example, the *blt1*Δ*1* mutant that lacks the N-terminal 79 residues of Blt1 was not concentrated at medial cortical nodes at endogenous expression levels, despite its strong localization to the cell periphery upon overexpression. Moreover, two constructs (*blt1*Δ*5* and *blt1*Δ*6*) lacking the C-terminal domain maintained localization to medial cortical nodes when expressed at endogenous levels, whereas we observed cytoplasmic localization for the *blt1*Δ*8* mutant, which truncates both the N- and C-terminal domains (Fig. 3; see also Fig. S6). We concluded that the N terminus of Blt1 gov-

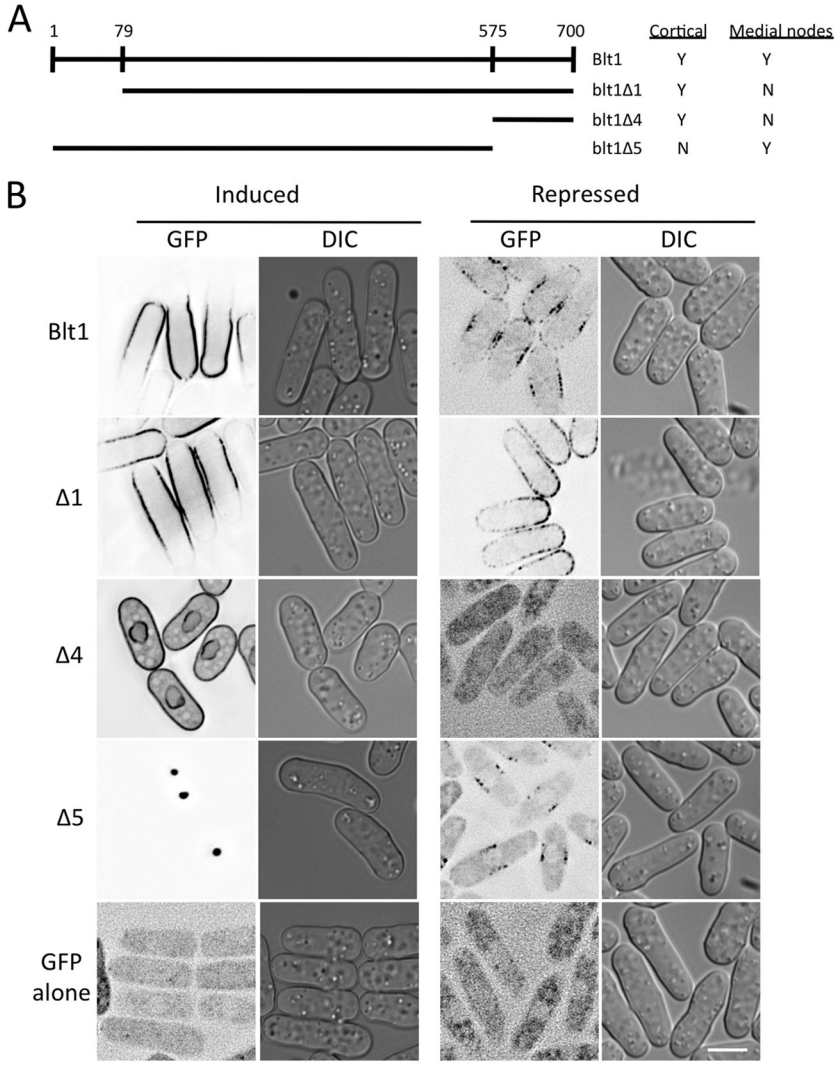

FIG 3 Domain analysis of Blt1. (A) Schematic of key truncation constructs. Right columns indicate whether the constructs localize to the cell cortex upon overexpression or to medial nodes upon low-level expression. Y, yes; N, no. A complete list of constructs and localization data are provided in Fig. S6 of the supplemental material. (B) Images of the Blt1 truncation constructs from panel A, expressed as GFP-fusion proteins in *blt1*Δ cells (strain JM429). Images are inverted single deconvolved focal planes with the accompanying DIC image. Overexpression was induced by removal of thiamine for 24 h; expression under repressed conditions was similar to endogenous Blt1 levels. Bar, 5 μm.

erns localization to medial cortical nodes, while a separable C-terminal domain may drive association with membrane lipids.

The Blt1 N terminus directs node localization and function. To further investigate the role of the Blt1 N terminus, we integrated the *blt1Δ1* truncation mutant with an mCherry tag under the control of the endogenous promoter as the sole copy in the genome. *blt1*Δ1-mCherry localized to the cell cortex asymetrically but did not colocalize with Cdr2-mEGFP in cortical nodes (Fig. 4A). This sharply contrasted with the colocalization of wild-type Blt1-mCherry with Cdr2-mEGFP and mimicked the localization defect observed for Blt1 in *cdr2*Δ cells. Indeed, the localization of Blt1-mCherry and blt1Δ1-mCherry was identical in *cdr2*Δ cells (Fig. 4B), indicating that this N-terminal domain is required for Blt1 recruitment to medial cortical nodes by Cdr2. In support of this conclusion, the physical interaction of Cdr2 and Blt1 by coimmunoprecipitation was reduced in the *blt1Δ1* mutant (see Fig. S7 in the supplemental material).

We next tested the function of the Blt1 N terminus in cortical recruitment of Mid1-Nter for cytokinesis. Cortical *blt1Δ1* failed to recruit Mid1-Nter to cortical nodes, in contrast to full-length Blt1 (Fig. 4C). Consistent with this defect in Mid1-Nter localization, we found that Gef2-mEGFP was absent from interphase cortical nodes of *blt1Δ1* cells and did not colocalize with blt1Δ1-mCherry at the cell cortex (see Fig. S7B in the supplemental material). This suggests that the N terminus of Blt1 is required for recruitment of Gef2 to interphase cortical nodes, and Gef2 then acts as an adaptor for Mid1-Nter. We note that Gef2 localized to the cytokinetic ring in *blt1Δ1* cells (see Fig. S7C), similar to *blt1*Δ cells (31), indicating an independent recruitment mechanism later in the cell cycle. The failure in recruitment of Gef2 and Mid1-Nter to medial cortical nodes led to functional defects, as the *blt1Δ1* mutation exhibited synthetic defects with *mid1-Nter* identical to *blt1*Δ (Fig. 4D). We concluded that the N terminus of Blt1 is required for Blt1 recruitment to cortical nodes by Cdr2 and subsequent recruitment of Gef2 and Mid1-Nter to the cell cortex.

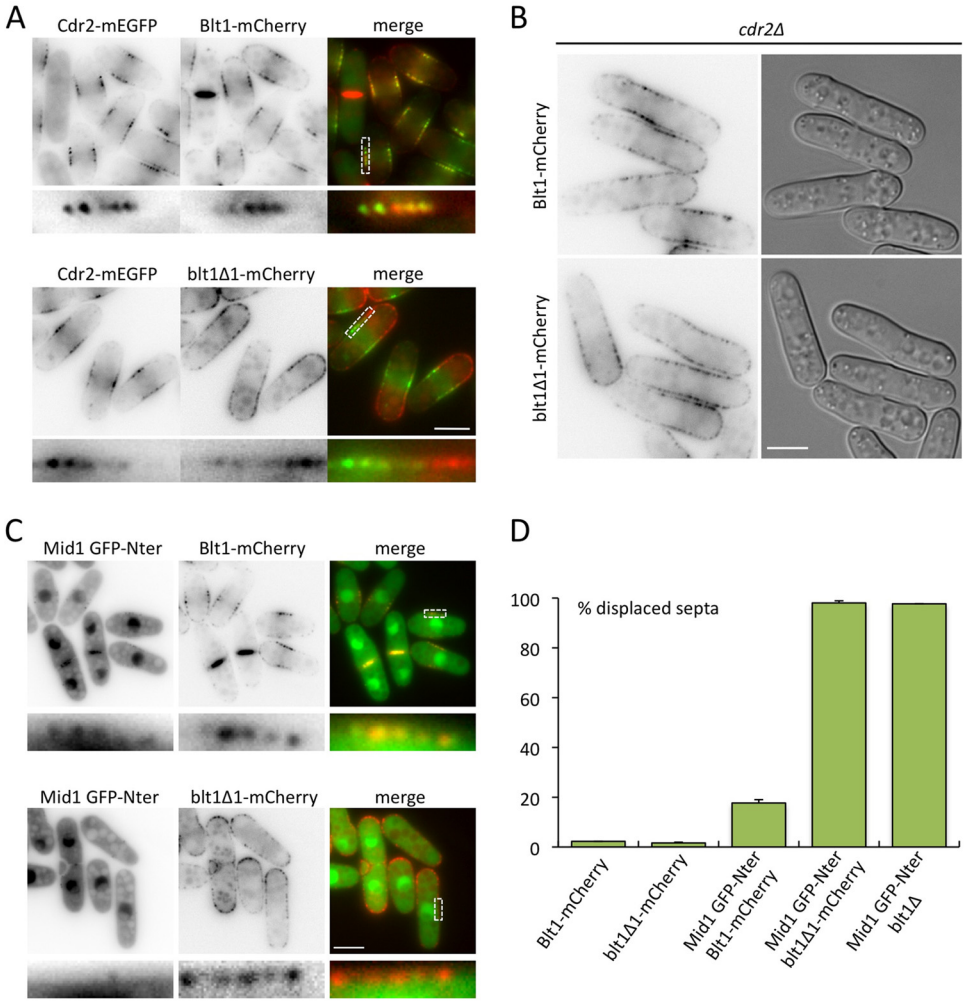

FIG 4 The N terminus of Blt1 is required for localization and function. (A) Cdr2-mEGFP colocalizes with Blt1-mCherry but not blt1Δ1-mCherry. Images are inverted single focal planes; bottom rows are magnified views of the white, boxed regions. Bar, 5 μm. Strains used were JM2193 and JM2194. (B) Localization of Blt1-mCherry and blt1Δ1-mCherry in *cdr2*Δ cells. Left images are inverted single focal planes; right images were produced by DIC. Bar, 5 μm. Strains used were JM2197 and JM2198. (C) Mid1 GFP-Nter colocalizes with cortical Blt1-mCherry but not blt1Δ1-mCherry. Images are presented as described for panel A. Bar, 5 μm. Strains used were JM1681 and JM1682. (D) Percentages of displaced septa for the indicated genotypes (strains JM1684, JM1685, JM1681, JM1682, and JM1680). Bars represent means ± standard deviations (error bars) from two separate experiments ($n > 200$ cells in each experiment).

The Blt1 C terminus associates with lipids to direct cortical localization. Our data suggest that Blt1 is recruited to cortical nodes by an N-terminal domain that associates with Cdr2, but it can independently target the cell cortex through a C-terminal domain that may interact with membrane lipids. To analyze the function of this Blt1 C-terminal domain in more detail, we integrated the *blt1*Δ*5* mutant, which lacks the C-terminal domain, with a GFP tag under the control of the endogenous promoter as the sole copy in the genome. Consistent with our plasmid-based results, *blt1*Δ*5*-mEGFP localized to medial cortical nodes despite lacking the membrane-binding domain (Fig. 5). However, this localization of *blt1*Δ*5*-mEGFP to the cell cortex was abolished in *cdr2*Δ cells (Fig. 5). This contrasted with full-length Blt1 and the *blt1*Δ*1* mutant, which both remained cortical in *cdr2*Δ cells (Fig. 4B). These data confirmed that Blt1 has separable domains to target medial cortical nodes versus the cortex in general.

We next tested the possibility that the Blt1 C terminus targets the cell cortex by binding to lipids. Cell extracts containing either full-length GFP-Blt1 or the truncated GFP-blt1Δ5 (see Fig. S8 in the supplemental material) were incubated with lipid array strips. Using anti-GFP antibodies, we found that Blt1 interacted with negatively charged phospholipids but *blt1*Δ*5* did not (Fig. 6A). This indicated that Blt1 is a membrane-binding protein, although we note that this interaction could be indirect. In support of a direct interaction with lipids, sequence analysis of the C-terminal domain revealed several clusters of positively charged residues that could facilitate association with negatively charged lipids in cellular membranes (Fig. 6B). Truncation of the C-terminal 26 residues, including two adjacent lysines, did not impair cortical localization. In contrast, truncation to delete additional clusters of basic residues abolished cortical localization (Fig. 6B and C). These data strongly suggest the possibility that basic residues in the C-terminal domain establish electrostatic interactions with negatively charged phospholipids to promote Btl1 cortical localization in cells.

Cortical targeting by the Blt1 C terminus is important for cytokinesis. Finally, we tested the role of the Blt1 C-terminal do-

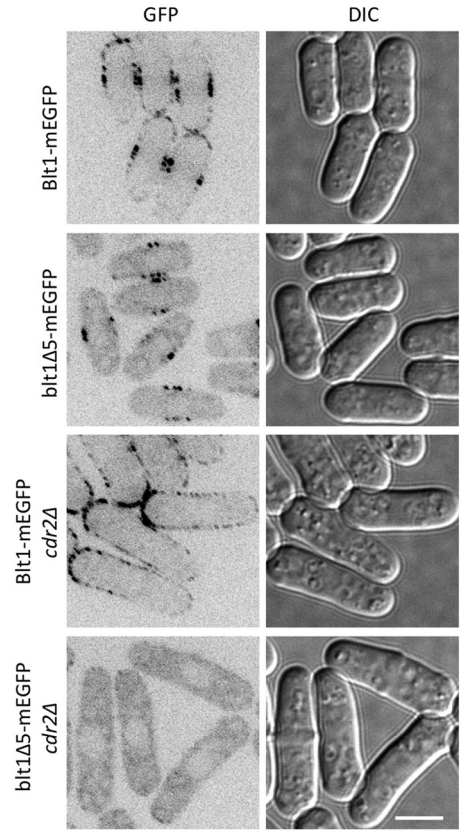

FIG 5 Cdr2 is required for cortical localization of blt1Δ5 but not full-length Blt1. Localization of endogenous Blt1 and truncated blt1Δ5 in wild-type and *cdr2*Δ cells. Images are inverted single confocal planes. Bar, 5 μm. Strains used were JM151, JM216, JM1607, and JM1642.

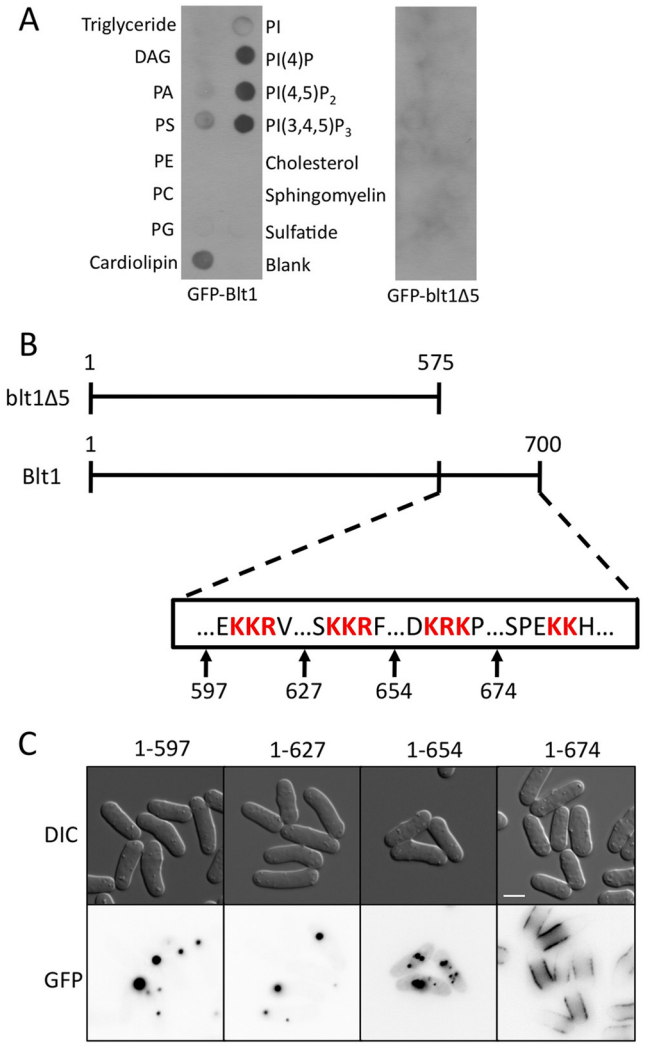

FIG 6 Blt1 interacts with lipids through a C-terminal domain. (A) Whole-cell extracts from cells overexpressing GFP-Blt1 or the truncated GFP-blt1Δ5 in strain JM429 were incubated with lipid strip arrays and analyzed by Western blotting using anti-GFP antibodies. (B) Schematic of truncated blt1Δ5 and full-length Blt1. Clusters of basic residues are highlighted. (C) Localization of the indicated constructs upon overexpression in *blt1*Δ cells. Bar, 5 μm. The strain used was JM429.

main in cytokinesis. Interestingly, we found that *blt1Δ5* recruited and colocalized with Mid1-Nter at medial cortical nodes during interphase (Fig. 7A). Thus, deleting the membrane-binding domains of both Mid1 and Blt1 did not prevent their coaccumulation at medial cortical nodes. This indicated that Blt1 acts as a scaffold, independent of its membrane-binding activity, to promote the robust localization of Mid1 at medial cortical nodes.

This result raised the possibility that the Blt1 C terminus is dispensable for function, because the Blt1 N terminus mediates localization to cortical nodes and downstream recruitment of Mid1-Nter. However, the *blt1Δ5* and *mid1-Nter* mutations exhibited strong synthetic defects in positioning the division plane (Fig. 7B and C). Truncating the C-terminal membrane-binding domain of either Mid1 or Blt1 did not lead to septation defects, but nearly all *blt1Δ5 mid1-Nter* double mutants displayed misplaced septa.

To determine the underlying mechanism that leads to septation defects in *blt1Δ5 mid1-Nter* cells, we used time-lapse microscopy of cells expressing Blt1-mEGFP or *blt1Δ5*-mEGFP. These cells also expressed the actomyosin ring marker Rlc1-mCherry and the spindle-pole body (SPB) marker Sfi1-mCherry. We observed the expected pattern of SPB separation and actomyosin ring assembly in *blt1Δ5* cells and only minor defects in *mid1-Nter* cells (Fig. 8A). In contrast, the double mutant displayed synthetic defects in spatial control of actomyosin ring assembly (Fig. 8A). Moreover, we observed that *blt1Δ5*-mEGFP rapidly detached from the cortex upon SPB separation, unlike full-length Blt1-mEGFP. The mutant *blt1Δ5*-mEGFP then reappeared as a large clump containing both *blt1Δ5*-mEGFP and Rlc1-mCherry (Fig. 8A, arrow heads). Mid1-Nter displayed similar behavior in early mitotic cells (see Fig. S9 [arrow heads] in the supplemental material). An actomyosin structure containing both Rlc1-mCherry and *blt1Δ5*-mEGFP assembled abnormally from these clumps, often resulting in elongated actomyosin filaments that reached the cell tips, reminiscent of the *mid1Δ* phenotype. These cytokinetic filaments at cell tips were only observed in the *blt1Δ5 mid1-Nter* double mutants (Fig. 8C). These results suggest that nodes containing *blt1Δ5* and Mid1-Nter are destabilized at mitotic entry in the absence of membrane binding by both Mid1 and Blt1. This lack of stability leads to defective recruitment of cytokinesis proteins, including myosin II, resulting in misplaced cytokinetic rings and septa.

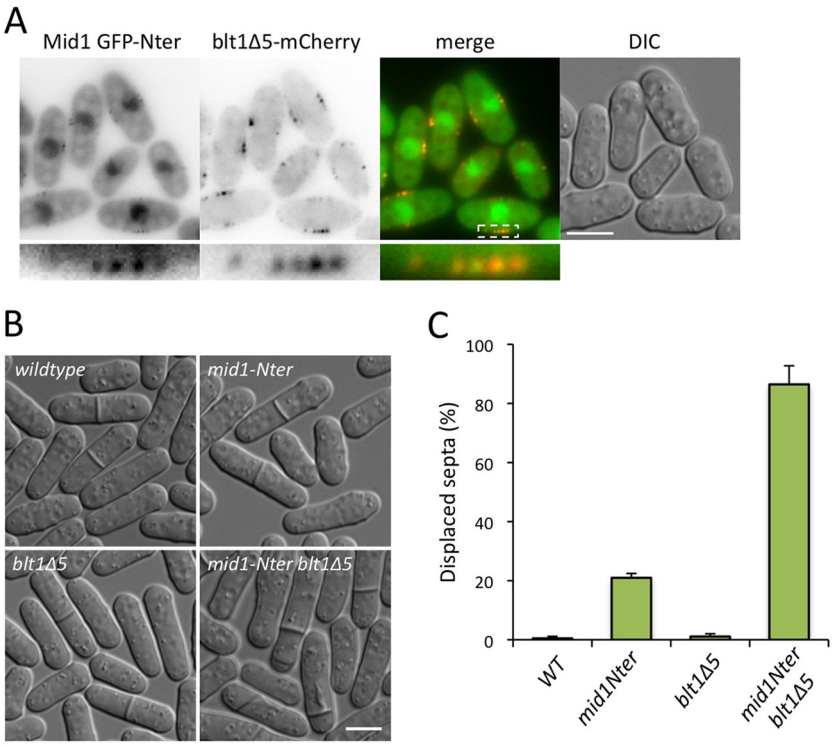

FIG 7 The Blt1 membrane-binding domain is required for Mid1-Nter function. (A) Mid1 GFP-Nter and Blt1Δ5-mCherry colocalize in cortical nodes. Images are inverted single deconvolved focal planes. The lower row is a magnified view of the boxed region. Bar, 5 μm. The strain used was JM1603 (B) DIC images of wild-type, *mid1-Nter*, *blt1Δ5-mCherry*, and *mid1-Nter blt1Δ5-mCherry* cells (strains JM1598, JM1603, JM1595, and JM1597). Bar, 5 μm. (C) Percentages of displaced septa in the indicated genotypes. Bars represent means ± standard deviations (error bars) from two separate experiments ($n > 200$ cells in each experiment). The strains used are the same as for panel B.

Why would *blt1Δ5 mid1-Nter* nodes dissociate from the cortex at mitotic entry? We considered a role for Cdr2, which recruits the *blt1Δ5* mutant to cortical nodes but dissociates from nodes at mitotic entry (10). During this stage, nodes mature by the recruitment of many cytokinesis proteins and then compact into a cytokinetic ring (5). If Cdr2 dissociation from nodes leads to detachment of *blt1Δ5* and Mid1-Nter, then constitutive tethering of Cdr2 to the cell cortex might suppress this defect. To test this prediction, we artificially tethered Cdr2 to the cell membrane by fusing the membrane-binding C-terminal fragment of Mod5 (containing basic residues and a CAAX prenylation motif) to the C terminus of Cdr2-GFP. Unlike wild-type Cdr2-GFP, this Cdr2-GFP-CAAX fusion protein was present at the cell cortex throughout cytokinesis (see Fig. S10 in the supplemental material). Consistent with our prediction, the addition of Cdr2-CAAX partially suppressed the septum-positioning defect of *blt1Δ5 mid1-Nter* double mutant cells (Fig. 9). We concluded that Cdr2 serves as the sole cortical anchor for cytokinetic nodes in these double mutant cells, and dissociation of Cdr2 from nodes during ring assembly leads to node detachment and cytokinesis defects.

DISCUSSION

Assembly of the contractile ring in fission yeast begins with the positioning of cortical nodes in the cell middle (1, 3, 5), followed by maturation and condensation of nodes into a contractile ring during mitosis. A similar process assembles the contractile ring in animal cells, where cytokinesis proteins are recruited to a broad equatorial band that subsequently condenses to form the mature actomyosin ring (32, 33). Our work provides molecular insight into the mechanisms that assemble and anchor cytokinetic nodes at the plasma membrane in fission yeast, with implications for cytokinetic ring assembly in a broad range of cell types.

We found that Blt1 acts as both a scaffold and a cortical anchor for the anillin-like protein Mid1, with Blt1-Mid1 interactions bridged by Gef2. The N terminus of Blt1 is required for localization to cortical nodes and for the recruitment of Gef2 and Mid1-Nter. It is currently unknown if Blt1 and Gef2 bind directly or indirectly, but we note that the C terminus of Gef2 is crucial for Gef2 interaction with nodes (31), raising the possibility that the Blt1 N terminus interacts with the Gef2 C terminus. We also note that additional uncharacterized proteins may facilitate these functional interactions. Scaffold proteins are emerging as key integrators of multicomponent systems, such as medial cortical nodes (34). In this scaffolding function, Blt1 may ensure robust assembly of the cell division machinery by integrating spatial and temporal information with physical connections to the cell cortex.

Blt1 scaffolding activity is independent from its interactions with the membrane, which depend on the C terminus. Several lines of evidence suggest that Blt1 may directly bind to lipids: (i) nonsaturable binding of Blt1 to the cortex upon overexpression; (ii) *in vitro* binding of Blt1-GFP but not truncated *blt1Δ5*-GFP to lipids in cell extracts; (iii) the presence of C-terminal basic-rich motifs with the potential to mediate the electrostatic interaction with acidic phospholipids, such as phosphatidylinositol 4,5-biphosphate [$PI(4,5)P_2$], enriched at the plasma membrane. Syn-

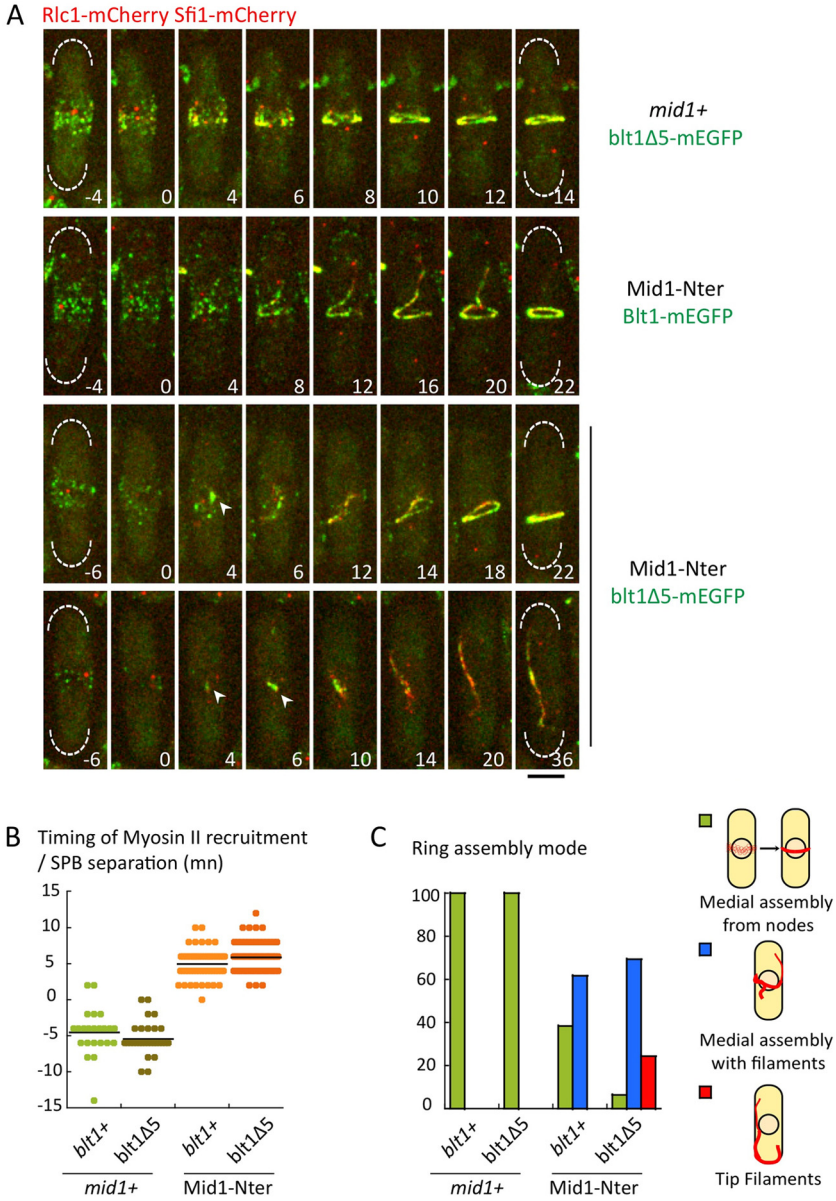

FIG 8 Cortical nodes disassemble during mitosis in *mid1-Nter blt1*Δ*5* cells. (A) Live cell imaging of the *mid1-Nter blt1*Δ*5-mEGFP* strain expressing the myosin II light chain Rlc1-mCherry and the SPB marker Sfi1-mRFP as a timer of mitotic entry (AP3925). mid1-Nter Blt1-mEGFP (AP3924) and *mid1*$^{+}$ *blt1*Δ*5-mEGFP* (AP3907) control strains are also shown. Note that at mitosis entry in the Blt1Δ5-mEGFP Mid1Nter mutant, Blt1Δ5-mEGFP nodes disappeared from the cortex, while large clusters containing both Blt1Δ5-mEGFP and Rlc1-mCherry assembled (arrow heads). The Rlc1-mCherry recruitment pattern was strongly affected. Images are maximum projections from spinning disc *z*-series. Bar, 5 μm. (B and C) Quantification of the timing of Rlc1-mCherry recruitment to nodes (B) and ring assembly mode (C). Measurements were performed using the same strains as for panel A and also a wild-type strain expressing the same markers (AP3906). Bars represent means ± standard deviations (error bars) from two separate experiments ($n > 200$ cells in each experiment).

thetic defects between the *blt1*Δ*5* and *mid1-Nter* mutants indicated that Blt1 interactions with the membrane act in parallel to the Mid1 membrane-binding helix.

Based on these results, we propose a model for the interactions between Mid1, Blt1, Gef2, Cdr2, and the plasma membrane within a node (Fig. 10). When membrane anchoring by both Mid1 and Blt1 is impaired, we propose that nodes remain cortical during interphase due to Cdr2, which may also facilitate interactions among Blt1, Gef2, and Mid1. However, Cdr2 leaves the cortex during mitosis, leading to node detachment and disassembly. Without proper cortical node attachment to the plasma membrane, the cytokinetic ring assembles from elongated clumps to generate severe cytokinesis defects. The formation of a clump-derived actomyosin filament in these cells resembles aberrant cytokinesis in *mid1*Δ mutants (35, 36). In support of our model, a Cdr2 construct artificially tethered to membranes during mitosis (Cdr2-GFP-CAAX) partially rescued the division plane definition defects of the *mid1-Nter blt1*Δ*5* double mutant. We note that the broader distribution of Cdr2-CAAX on the cortex compared to Cdr2 (see Fig. S10 in the supplemental material) may preclude a complete rescue.

Our model accounts for the phenotypes that we have de-

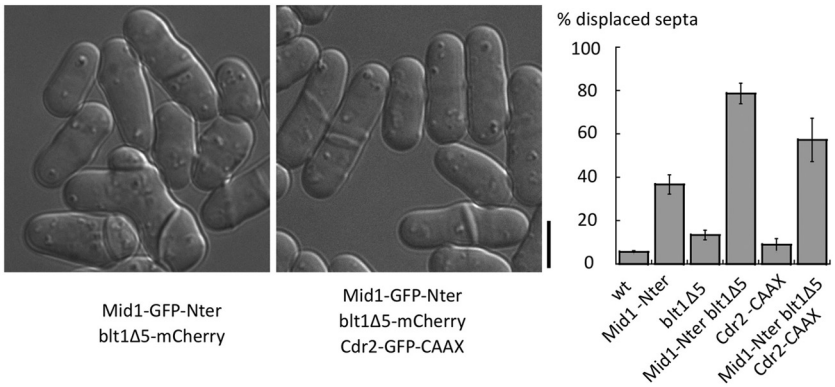

FIG 9 Cdr2-GFP-CAAX partially rescues septum-positioning defects in the *mid1-Nter blt1Δ5* mutant. DIC images (left) and percentages of displaced septa (right) in *Mid1-GFP-Nter* (AP998), *blt1Δ5-mCherry* (JM1597), *Mid1-GFP-Nter blt1Δ5-mCherry* (JM1603), *Cdr2-GFP-CAAX* (AP3898), and *Mid1-GFP-Nter Blt1Δ5-mCherry Cdr2-GFP-CAAX* (AP3909) strains are shown. Bars represent means ± standard deviations (error bars) from three separate experiments (n = 300 cells in each experiment).

scribed, but more complex relationships are likely to exist in cells. For example, in *mid1*(Δ300-350) and *gef2Δ* mutants, Blt1 is less concentrated in medial nodes (see Fig. S3 in the supplemental material), indicating bidirectional regulation or feedback in the assembly of these structures. These nodes also contain additional proteins, including the kinesin-like protein Klp8 and the membrane-binding F-BAR protein Cdc15, with physical links to the Blt1-Mid1-Gef2-Cdr2 module (11). Further, multiple copies of these proteins are present in each node, and oligomerization and multivalent interactions are likely to generate more complex, higher-order structures. We anticipate that additional proteins and interactions will be uncovered in future work on these cortical node structures.

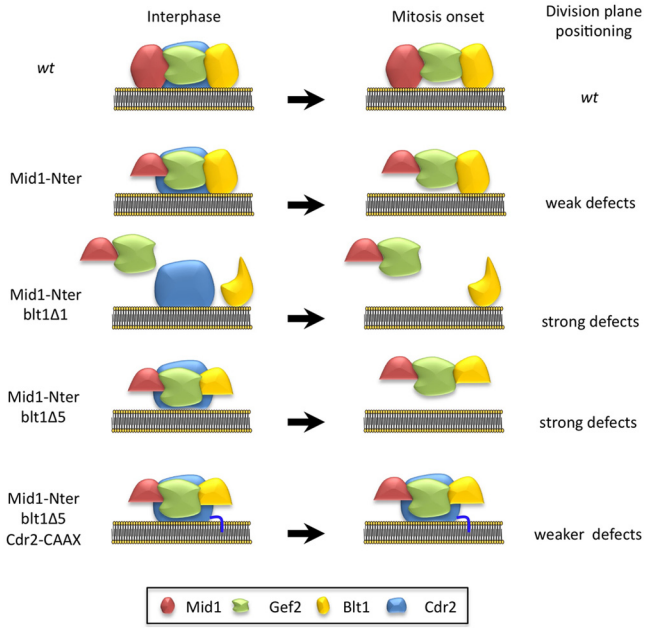

FIG 10 Model of proposed molecular interactions in medial cortical nodes. During interphase, Cdr2 recruits Mid1 and Blt1 to medial cortical nodes. Gef2 reinforces the stability of the complex by mediating additional Mid1-Blt1 indirect interactions. Cortical anchoring of the complex is ensured in a redundant manner by Cdr2, Blt1, and Mid1. The Blt1 N terminus, deleted in the *blt1Δ1* mutant, controls Blt1 recruitment to cortical nodes and subsequent recruitment of Gef2 and Mid1-Nter, which is deficient for membrane binding. The Blt1 C terminus, deleted in *blt1Δ5*, acts as a membrane anchor for Blt1. The interactions of Mid1 and Blt1 with membranes are dispensable for recruitment of Mid1-Gef2-Blt1 to nodes during interphase due to association with Cdr2. However, Cdr2 dissociation from the cortex during mitosis creates a requirement for membrane binding by either Mid1 or Blt1. At this stage, cortical nodes in the double mutant *mid1-Nter blt1Δ5* dissociate from the cortex, leading to division plane-positioning defects. Artificial node anchoring during mitosis by Cdr2-CAAX can partially suppress these defects. Note that protein interactions in the model may be indirect and involve additional factors.

We note that Blt1 is necessary for Gef2 association with medial cortical nodes during interphase (11), but Gef2 localizes to the cytokinetic ring independently of Blt1 during mitosis (31). Accordingly, we found that Gef2 localized to the contractile ring in *blt1Δ1* cells but not with medial cortical nodes during interphase (see Fig. S7C in the supplemental material). In contrast, *gef2Δ* cells display a lack of Mid1-Nter at the contractile ring (31) and decreased levels of Blt1 at the contractile ring (see Fig. S11 in the supplemental material). These results suggest that Gef2 may be independently recruited to the assembled contractile ring by other factors to promote Mid1-Nter and Blt1 recruitment. Further work is necessary to resolve the underlying molecular mechanisms.

The overlapping roles of the Blt1 and Mid1 membrane-binding domains highlight the importance of stable attachment of structures such as nodes to the plasma membrane. During contractile ring assembly, medial cortical nodes mature by sequentially recruiting components of the contractile ring, while Cdr2 dissociates from nodes. Cortical nodes become mobile within the cell cortex at this stage, driving assembly of the mature cytokinetic ring (4, 5). We found that interactions of Blt1 and Mid1 with the membrane are crucial in this time frame. This suggests that multiple connections to membrane lipids may stabilize node attachment to the plasma membrane during dynamic node movements.

Animal cells undergo a similar process, where cytokinesis factors, including the Mid1-like protein anillin, are initially recruited to a broad equatorial band that subsequently condenses into a compact ring (32, 33). As in fission yeast, overlapping membrane anchors may be required to ensure movement of these multiprotein assemblies within the plane of the cell cortex. It is interesting that Blt1 associates with negatively charged phospholipids, including $PI(4,5)P_2$, which recruits the Mid1-like protein anillin to the central cortex during animal cell cytokinesis (37). This sug-

gests that similar interactions between proteins and lipids may underlie the robust assembly of the cytokinetic ring in diverse cell types and organisms.

A separate role for membrane-binding domains may be the spatial organization of phospholipids in the membrane. The Blt1 membrane-binding domain associates with negatively charged phospholipids, such as $PI(4,5)P_2$, which acts as a signaling molecule during cytokinesis (38). Thus, membrane-binding domains may also promote signaling pathways through the recruitment and/or retention of specific lipids. A growing number of protein-protein and protein-lipid interactions are being uncovered in the cytokinetic ring (2, 4, 5). By defining the physical interactions within cytokinetic ring precursors, such as cortical nodes, we anticipate the discovery of additional mechanisms that promote proper positioning and assembly of the cell division machinery. These interactions between protein and lipid components of the cytokinetic ring drive the dynamic events that ensure faithful cycles of cell division.

ACKNOWLEDGMENTS

We thank P. Nurse for support and C. Dupre for technical assistance in the early stages of this work. We thank J.-Q. Wu and K. Gould for strains and Sergio Rincon for production of the Cdr2-CAAX strain and for critical reading of the manuscript.

This work was supported by the Hitchcock Foundation, by National Institutes of Health grants P30GM092357 and 1R01GM099774 (J.B.M.), by Agence Nationale de la Recherche, Ligue Nationale Contre le Cancer (Programme Labellisation), and Programme Emergence, Mairie de Paris. J.B.M. is a Pew Scholar in the Biomedical Sciences. M.A. received a fellowship from Association pour la Recherche contre le Cancer. M.G.-V. received a Ph.D. fellowship from Université Paris-Sud.

REFERENCES

1. **Almonacid M, Paoletti A.** 2010. Mechanisms controlling division-plane positioning. Semin. Cell Dev. Biol. **21**:874–880.
2. **Glotzer M.** 2005. The molecular requirements for cytokinesis. Science **307**:1735–1739.
3. **Oliferenko S, Chew TG, Balasubramanian MK.** 2009. Positioning cytokinesis. Genes Dev. **23**:660–674.
4. **Pollard TD.** 2010. Mechanics of cytokinesis in eukaryotes. Curr. Opin. Cell Biol. **22**:50–56.
5. **Pollard TD, Wu JQ.** 2010. Understanding cytokinesis: lessons from fission yeast. Nat. Rev. Mol. Cell Biol. **11**:149–155.
6. **Chang F, Woollard A, Nurse P.** 1996. Isolation and characterization of fission yeast mutants defective in the assembly and placement of the contractile actin ring. J. Cell Sci. **109**:131–142.
7. **Sohrmann M, Fankhauser C, Brodbeck C, Simanis V.** 1996. The dmf1/mid1 gene is essential for correct positioning of the division septum in fission yeast. Genes Dev. **10**:2707–2719.
8. **Almonacid M, Moseley JB, Janvore J, Mayeux A, Fraisier V, Nurse P, Paoletti A.** 2009. Spatial control of cytokinesis by Cdr2 kinase and Mid1/anillin nuclear export. Curr. Biol. **19**:961–966.
9. **Celton-Morizur S, Racine V, Sibarita JB, Paoletti A.** 2006. Pom1 kinase links division plane position to cell polarity by regulating Mid1p cortical distribution. J. Cell Sci. **119**:4710–4718.
10. **Morrell JL, Nichols CB, Gould KL.** 2004. The GIN4 family kinase, Cdr2p, acts independently of septins in fission yeast. J. Cell Sci. **117**:5293–5302.
11. **Moseley JB, Mayeux A, Paoletti A, Nurse P.** 2009. A spatial gradient coordinates cell size and mitotic entry in fission yeast. Nature **459**:857–860.
12. **Padte NN, Martin SG, Howard M, Chang F.** 2006. The cell-end factor pom1p inhibits mid1p in specification of the cell division plane in fission yeast. Curr. Biol. **16**:2480–2487.
13. **Martin SG, Berthelot-Grosjean M.** 2009. Polar gradients of the DYRK-family kinase Pom1 couple cell length with the cell cycle. Nature **459**:852–856.
14. **Almonacid M, Celton-Morizur S, Jakubowski JL, Dingli F, Loew D, Mayeux A, Chen JS, Gould KL, Clifford DM, Paoletti A.** 2011. Temporal control of contractile ring assembly by Plo1 regulation of myosin II recruitment by Mid1/anillin. Curr. Biol. **21**:473–479.
15. **Bezanilla M, Wilson JM, Pollard TD.** 2000. Fission yeast myosin-II isoforms assemble into contractile rings at distinct times during mitosis. Curr. Biol. **10**:397–400.
16. **Coffman VC, Nile AH, Lee IJ, Liu H, Wu JQ.** 2009. Roles of formin nodes and myosin motor activity in Mid1p-dependent contractile-ring assembly during fission yeast cytokinesis. Mol. Biol. Cell **20**:5195–5210.
17. **Laporte D, Coffman VC, Lee IJ, Wu JQ.** 2011. Assembly and architecture of precursor nodes during fission yeast cytokinesis. J. Cell Biol. **192**:1005–1021.
18. **Motegi F, Mishra M, Balasubramanian MK, Mabuchi I.** 2004. Myosin-II reorganization during mitosis is controlled temporally by its dephosphorylation and spatially by Mid1 in fission yeast. J. Cell Biol. **165**:685–695.
19. **Padmanabhan A, Bakka K, Sevugan M, Naqvi NI, D'Souza V, Tang X, Mishra M, Balasubramanian MK.** 2011. IQGAP-related Rng2p organizes cortical nodes and ensures position of cell division in fission yeast. Curr. Biol. **21**:467–472.
20. **Wu JQ, Kuhn JR, Kovar DR, Pollard TD.** 2003. Spatial and temporal pathway for assembly and constriction of the contractile ring in fission yeast cytokinesis. Dev. Cell **5**:723–734.
21. **Wu JQ, Pollard TD.** 2005. Counting cytokinesis proteins globally and locally in fission yeast. Science **310**:310–314.
22. **Celton-Morizur S, Bordes N, Fraisier V, Tran PT, Paoletti A.** 2004. C-terminal anchoring of mid1p to membranes stabilizes cytokinetic ring position in early mitosis in fission yeast. Mol. Cell. Biol. **24**:10621–10635.
23. **Moreno S, Klar A, Nurse P.** 1991. Molecular genetic analysis of fission yeast Schizosaccharomyces pombe. Methods Enzymol. **194**:795–823.
24. **Keeney JB, Boeke JD.** 1994. Efficient targeted integration at leu1-32 and ura4-294 in Schizosaccharomyces pombe. Genetics **136**:849–856.
25. **Paoletti A, Chang F.** 2000. Analysis of mid1p, a protein required for placement of the cell division site, reveals a link between the nucleus and the cell surface in fission yeast. Mol. Biol. Cell **11**:2757–2773.
26. **Bahler J, Wu JQ, Longtine MS, Shah NG, McKenzie A, III, Steever AB, Wach A, Philippsen P, Pringle JR.** 1998. Heterologous modules for efficient and versatile PCR-based gene targeting in Schizosaccharomyces pombe. Yeast **14**:943–951.
27. **Hentges P, Van Driessche B, Tafforeau L, Vandenhaute J, Carr AM.** 2005. Three novel antibiotic marker cassettes for gene disruption and marker switching in Schizosaccharomyces pombe. Yeast **22**:1013–1019.
28. **Snaith HA, Sawin KE.** 2003. Fission yeast mod5p regulates polarized growth through anchoring of tea1p at cell tips. Nature **423**:647–651.
29. **Craven RA, Griffiths DJ, Sheldrick KS, Randall RE, Hagan IM, Carr AM.** 1998. Vectors for the expression of tagged proteins in Schizosaccharomyces pombe. Gene **221**:59–68.
30. **Kabeche R, Baldissard S, Hammond J, Howard L, Moseley JB.** 2011. The filament-forming protein Pil1 assembles linear eisosomes in fission yeast. Mol. Biol. Cell **22**:4059–4067.
31. **Ye Y, Lee IJ, Runge KW, Wu JQ.** 2012. Roles of putative Rho-GEF Gef2 in division-site positioning and contractile-ring function in fission yeast cytokinesis. Mol. Biol. Cell **23**:1181–1195.
32. **D'Avino PP.** 2009. How to scaffold the contractile ring for a safe cytokinesis - lessons from Anillin-related proteins. J. Cell Sci. **122**:1071–1079.
33. **Green RA, Paluch E, Oegema K.** 2012. Cytokinesis in animal cells. Annu. Rev. Cell Dev. Biol. **28**:29–58.
34. **Good MC, Zalatan JG, Lim WA.** 2011. Scaffold proteins: hubs for controlling the flow of cellular information. Science **332**:680–686.
35. **Hachet O, Simanis V.** 2008. Mid1p/anillin and the septation initiation network orchestrate contractile ring assembly for cytokinesis. Genes Dev. **22**:3205–3216.
36. **Huang Y, Yan H, Balasubramanian MK.** 2008. Assembly of normal actomyosin rings in the absence of Mid1p and cortical nodes in fission yeast. J. Cell Biol. **183**:979–988.
37. **Liu J, Fairn GD, Ceccarelli DF, Sicheri F, Wilde A.** 2012. Cleavage furrow organization requires PIP_2-mediated recruitment of anillin. Curr. Biol. **22**:64–69.
38. **Brill JA, Wong R, Wilde A.** 2011. Phosphoinositide function in cytokinesis. Curr. Biol. **21**:R930–R934.